INTERNATIONAL JOURNAL FOR NUMERICAL METHODS IN FLUIDS
Int. J. Numer. Meth. Fluids 2002; **40**:253–261 (DOI: 10.1002/fld.275)

The numerical simulation of unsteady heat conduction in a premature infant

M. Breuß[1,*], B. Fischer[2] and A. Meister[1]

[1] *Department of Mathematics, Center for Differential Equations and Dynamical Systems, University of Hamburg, Germany*
[2] *Department of Mathematics, Medical University of Lübeck, Germany*

SUMMARY

This paper presents a mathematical model for time-dependent heat transfer processes in a premature infant as well as a finite volume scheme for the numerical solution of the underlying equations. The modelling of important physiological processes leads to a bio-heat equation. The main property of this formulation is the time-dependent heat distribution by blood flow. The employed finite volume scheme relies on the use of unstructured grids. Numerical simulations are presented which show the development of physical states due to a change in boundary values. Copyright © 2002 John Wiley & Sons, Ltd.

KEY WORDS: unsteady heat conduction; premature infants; numerical simulation; unstructured grids; finite volume method

1. INTRODUCTION

Severe asphyxia is an important cause for injuries of the developing brain [1]. Experimental studies have shown that the neuronal loss happens over a period of several days after such an incident [2]. One of the factors that influence the degree and distribution of neuronal loss is the cerebral temperature. Clinical studies have shown that lowering the cerebral temperature can prevent much damage [3]. The question arises, if the cerebral temperature of a premature infant can be lowered by manipulating the environmental conditions inside an incubator while the rest of the body maintains a pleasant temperature.

It is useful to discuss some medical aspects concerning premature infants. This is done in Section 2. Since it is an important question how fast a useful thermal state within the body can be achieved without dealing only with steady states, it makes sense to investigate the temporal evolution of the whole process. Section 3 deals with the governing equations of our instationary model. Since the thermal maturity of an infant can be related to its size, the model has to be applicable to different size neonates in order to be of practical importance. This is done by employing unstructured grids within a finite volume framework. In Section 4,

* Correspondence to: M. Breuß, FB Mathematik, Universitat Hamburg, Bunesstrasse, 20156 Hamburg, Germany.

Received May 2001
Revised September 2001

we briefly outline the used technique. Finally, we present the results of simulations using available real life data in Section 5.

2. ASPECTS OF THE MODEL

In order to show that our aim is not to work on an academic problem, we have to make some comments on our approach. Due to ethical and also technical reasons it is not possible to observe the temperature distribution within the brain of premature infants in the required detail. This is also true in the case of adults. Concerning adults a large amount of statistical data is available, but by the known differences in physiology and anatomy between adults and premature infants it is impossible to derive valid statements based on that information for the case we are interested in. Additionally, the mutual effects between different physiological processes which are responsible for heat transfer within the body are medically not well understood up to now. Because of this, there is no medical background on which an accurate statement can be made for the described situation. Therefore, a mathematical model is needed covering different known aspects in order to get an insight into the corresponding real world process.

Mathematical models for human thermoregulation already exist in the literature for the case of adults, see e.g. References [4–7]. However, these models are not applicable in the situation this paper is concerned with because of the differences in the physiological and anatomical attributes of adults and premature infants. For a description of these differences which have a strong effect on the whole modelling process see, e.g. References [4, 8]. In the described situation, a model is helpful if we demand from it that it includes models for the thermoregulators of the body, that it includes a model for the thermal maturity and that it gives detailed results for temperature profiles within the head. Up to now, multi-dimensional models of premature infants which include thermoregulative aspects do not exist with the exception of the model investigated by Fischer *et al.* [9], but that model relies on a steady-state assumption.

The term thermoregulation stands for the active measurements of the body to hold a neutral temperature. One of the main regulators are the vital organs including especially the brain, which can be a reason why a selective cooling of the brain may not be successful. Another significant heat source are the muscles directly in connection with the skeleton. The most important possibility for the body to loose heat is through the skin. Additionally, the blood flow has to be taken into account.

In the case of adults, the thermoregulative functions are fully developed and the idea of selectively cooling the brain does not make sense. Concerning premature infants, the situation is totally different. First, the possibility to loose heat through the skin is dramatically increased since the surface to volume ratio is three times as high as the ratio of an adult. Second, the isolating fat layer directly under the skin is very thin and the heat conductivity of the premature body is higher than the heat conductivity of the body of the adult. As a result, the temperature within premature infants can easily be influenced by the environment. Another aspect is that the rate of thermoregulative reactions of the body cannot increase as much in the case of a premature infant as in the case of a more mature infant or an adult if the temperature is lowered from outside. This fact is referred to as the thermal maturity of the infant.

We implement these aspects as follows. The dynamic changes in the heat distribution are modelled by a so-called bio-heat equation. Concerning the boundary conditions we assume that it is possible to exert sufficient control on the environmental parameters inside an incubator

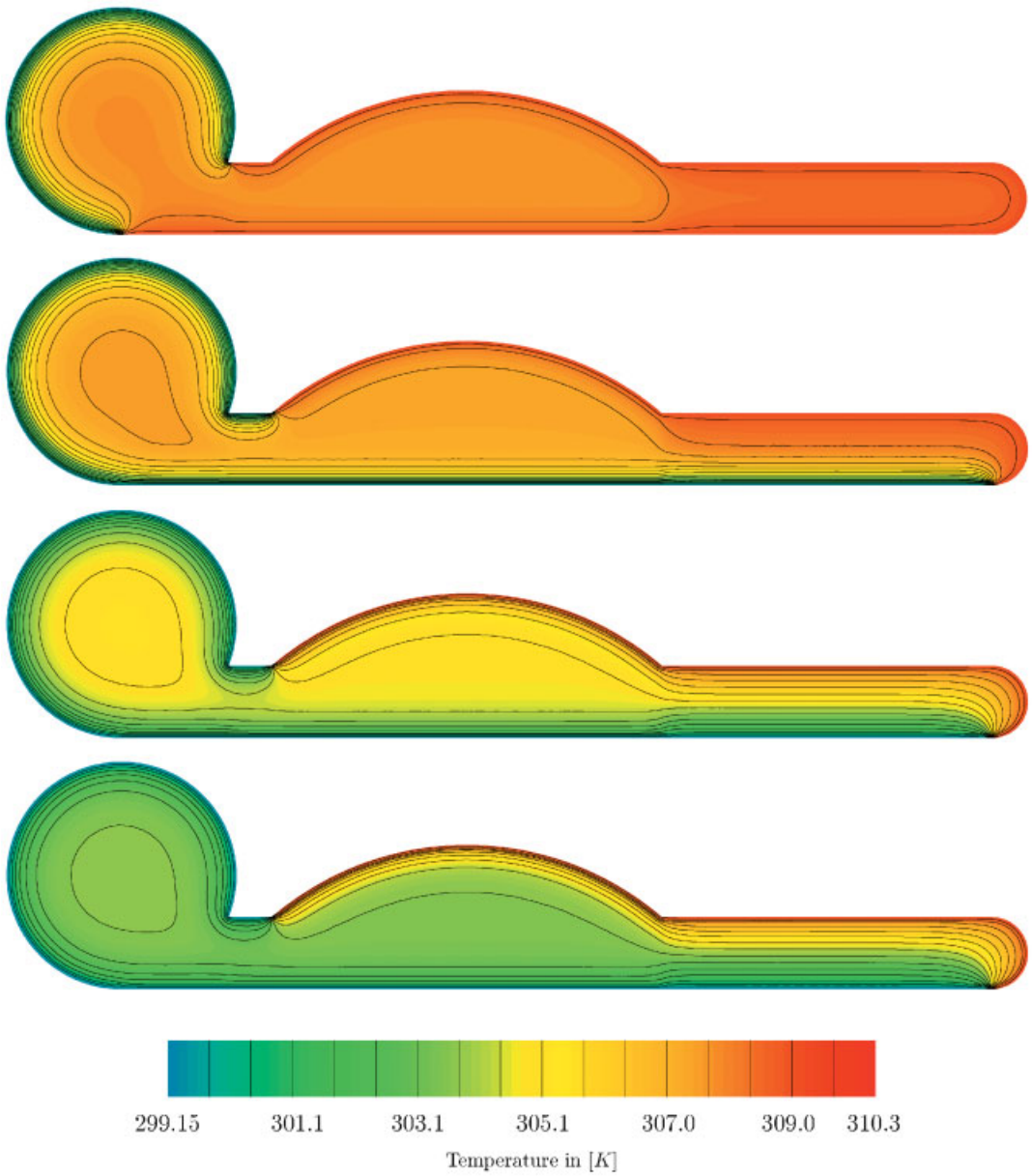

Plate 1. Evolution of the temperature distribution for the described case.

so that the definition of a boundary temperature at the skin of the infant makes sense, i.e. we employ Dirichlet conditions with respect to temperature which is a plausible assertion as well as a modelling step. Since the thermal maturity can be linked to the size of the infant it is implemented via the geometry. This is especially important since the geometry strongly influences the validity of computed temperature profiles [10]. Corresponding values for the involved parameters of metabolical heat production can be defined by results of clinical studies, see e.g. References [4, 11, 12].

All the works concerning thermoregulation of adults deal with empirical situations in the sense that the described models focus on the effects of roughly resumed environmental influences on an average grown up human, i.e. they deal with the effects of particularly hot, cold or otherwise special environmental conditions. The underlying application typically deals with empirical situations, e.g. the effects of extremely hot working conditions are addressed in order to prevent long-term health problems of industrial workers. See Reference [13] for a description of typical applications. In contrast, our scheme has to be applicable to infants of different sizes with accordingly different physiological behaviour because of the different maturity of premature infants of different age, and so unstructured grids have to be used. Additionally, we consider different tissues (bone, fat, skin and kernel) which feature different coefficients for heat conductivity and metabolical rates. For a detailed description we refer to Reference [9]. Another distinctive feature of our model is that heat transfer can take place by a model for bloodflow, see also Reference [14] for a discussion of that topic.

Our model is an extension of the model used by Fischer *et al.* which relies on a steady state assumption [9]. We extend the model to the unsteady case which results in the possibility to investigate numerical solutions which are not in a steady state but which have a physical meaning. As a result of this, time dependent boundary conditions can be employed in order to investigate changes in the temperature distribution due to dynamic changes in the environment. As an important aspect, it is perhaps possible based on the knowledge of predictable intermediate states to define a control mechanism or a sequence of boundary conditions which ensure that a desired state of the temperature distribution within a considered infant can be achieved after less time than in the case of constant boundary temperatures.

3. GOVERNING EQUATIONS

The heat transfer within a body of the premature infant is modelled by the so-called bio-heat equation

$$c(\mathbf{x})\rho(\mathbf{x})\frac{\partial}{\partial t}T(\mathbf{x},t) = \operatorname{div}[\lambda(\mathbf{x})\nabla_{\mathbf{x}}T(\mathbf{x},t)] + f(\mathbf{x},t) \tag{1}$$

with the spatial variable $\mathbf{x} = (x_1, x_2)^{\mathrm{T}}$ and the temporal variable t. Thereby, we also have the temperature T, the heat conductivity of the tissue λ, the specific heat capacity of the tissue c and the density of the tissue ρ. With f we denote sources due to metabolic heat production and blood flow. This source term takes the form $f(\mathbf{x},t) = Q_{\mathrm{M}}(\mathbf{x}) + Q_{\mathrm{B}}(\mathbf{x},t)$. Thereby, we have the metabolic heat production Q_{M} and heat transfer due to bloodflow Q_{B}. While Q_{M} is a local heat source depending on the underlying tissue and the location in the body which can be defined directly by the use of available medical data [4, 12], the source term Q_{B} involves a further modelling step which is presented at the end of this section.

In Reference [9], Equation (1) was solved numerically under a steady-state assumption. Therefore, Fischer *et al.* [9] used a simplification of (1), namely

$$\frac{\partial}{\partial t} T(\mathbf{x},t) = \operatorname{div}[\lambda(\mathbf{x})\nabla_{\mathbf{x}} T(\mathbf{x},t)] + f(\mathbf{x},t), \tag{2}$$

where the density and the specific heat capacity of the tissue are omitted. In the cause of that simplified ansatz, a stationary model for the bloodflow was applied. As a result of this, one can conclude that the intermediate numerical results computed with the help of that stationary model are a sequence of 'quasi-equilibrium' states converging to an equilibrium situation.

We illustrate the difference between the model used by Fischer *et al.* and our extension as follows. In order to apply a finite volume strategy, it is useful to write the governing equation in divergence form. The governing equation describing the temporal evolution of the temperature in a physically sensible manner reads

$$\frac{\partial}{\partial t} T(\mathbf{x},t) = \frac{1}{c(\mathbf{x})\rho(\mathbf{x})} \operatorname{div}[\lambda(\mathbf{x})\nabla_{\mathbf{x}} T(\mathbf{x},t)] + \frac{1}{c(\mathbf{x})\rho(\mathbf{x})} f(\mathbf{x},t). \tag{3}$$

The difference to Equation (2) used for the steady-state calculations is given by the factor $1/(c(\mathbf{x})\rho(\mathbf{x}))$. We especially notice that the first term on the right-hand side of (3) is not in divergence form with respect to the variable T anymore and so the intermediate states feature unphysical heat sources at the bordering elements of the spatial discretization between different tissues due to the spatial dependence of c and ρ. Since e.g. the specific heat capacity of the kernel is 3770 J/kg K and the specific heat capacity of bone is 2170 J/kg K while the specific densities of kernel and bone are nearly the same for our purpose, this difference is quite significant.

We now investigate the original equation (1) without a simplification. Let σ be an arbitrary control volume within our domain of interest D. Integration over σ gives

$$\int_{\sigma} c(\mathbf{x})\rho(\mathbf{x}) \frac{\partial T(\mathbf{x},t)}{\partial t} \,\mathrm{d}x = \int_{\partial\sigma} \lambda(\mathbf{x})\nabla_{\mathbf{x}} T(\mathbf{x},t) \,\mathrm{d}\mathbf{s} + \int_{\sigma} f(\mathbf{x},t) \,\mathrm{d}\mathbf{x}. \tag{4}$$

Assuming that the control volume σ does not change with time, the left-hand side of (4) gives

$$\int_{\sigma} c(\mathbf{x})\rho(\mathbf{x}) \frac{\partial T(\mathbf{x},t)}{\partial t} \,\mathrm{d}\mathbf{x} = \frac{\mathrm{d}}{\mathrm{d}t}\left[\int_{\sigma} c(\mathbf{x})\rho(\mathbf{x})T(\mathbf{x},t) \,\mathrm{d}\mathbf{x}\right],$$

which means that for each cell we get an expression for the temporal evolution of the quantity $\bar{T}(\mathbf{x},t) := c(\mathbf{x})\rho(\mathbf{x})T(\mathbf{x},t)$. We now choose to write Equation (1) in terms of the variable $\bar{T}$ and to investigate the evolution of this quantity since we already have divergence form in the first term on the right-hand side of (1). For abbreviation, we write $k(\mathbf{x}) := c(\mathbf{x})\rho(\mathbf{x})$ and we omit the notation of the variables $\mathbf{x} = (x_1, x_2)^{\mathrm{T}}$ and t. It is simple to write Equation (1) in the form

$$\partial_t \bar{T} = \partial_{x_1}[\lambda \partial_{x_1} T] + \partial_{x_2}[\lambda \partial_{x_2} T] + f. \tag{5}$$

Now we have to eliminate T in favour of $\bar{T}$. Equation (5) gives

$$\partial_t \bar{T} = \frac{\partial_{x_1}\lambda}{k} k\partial_{x_1} T + \frac{\lambda}{k} k\partial_{x_1}^2 T + \frac{\partial_{x_2}\lambda}{k} k\partial_{x_2} T + \frac{\lambda}{k} k\partial_{x_2}^2 T + f. \tag{6}$$

Because k depends on $\mathbf{x}$, getting k across ∂_i is a bit work. After a lengthy but simple computation, the divergence form in the new variable $\bar{T}$ reads

$$\partial_t \bar{T} = \nabla \cdot \left[\frac{\lambda}{k} \nabla \bar{T} - \frac{\lambda \bar{T}}{k^2} \nabla k \right] + f. \tag{7}$$

By Equation (7), it is evident that the formal change in the variable has the effect of an additional source term depending on ∇k.

We now constitute the bloodflow model. It is based on the assumption that there is a central bloodpool from which arterial blood is distributed with the temperature $T_B(t)$ into the body. There the temperature of the blood is locally influenced by the temperature of the tissue and *vice versa*. After that, the blood flows back through the veins into the bloodpool. This blood has the temperature $T_V(t)$. By this assumption, we get the equation

$$m_B c_B \frac{\mathrm{d}}{\mathrm{d}t} T_B(t) = \int_D \rho_B c_B K_B(\mathbf{x}) B(\mathbf{x}) \, \mathrm{d}\mathbf{x} [T_V(t) - T_B(t)] \tag{8}$$

for the temporal evolution of the bloodpool temperature T_B. Thereby, we denote by m_B the mass of the blood, by ρ_B the specific density of the blood, by c_B the specific heat capacity of the blood and by $K_B B$ the effective bloodflow which also influences T_V by

$$T_V(t) = \frac{\int_D K_B(\mathbf{x}) B(\mathbf{x}) T(\mathbf{x}, t) \, \mathrm{d}\mathbf{x}}{\int_D K_B(\mathbf{x}) B(\mathbf{x}) \, \mathrm{d}\mathbf{x}}. \tag{9}$$

This proceeding constitutes the source term Q_B as

$$Q_B(\mathbf{x}, t) = \rho_B c_B K_B(\mathbf{x}) B(\mathbf{x}) [T_B(t) - T(\mathbf{x}, t)]. \tag{10}$$

We shortly investigate some properties of the bloodflow model in order to clarify the subject. Therefore, let the abbreviations

$$\alpha = \rho_B c_B, \qquad \beta = \int_D K_B(\mathbf{x}) B(\mathbf{x}) \, \mathrm{d}\mathbf{x} \quad \text{and} \quad \gamma = \rho_B / m_B$$

hold. Then it follows directly from (8) that we can write

$$\frac{\mathrm{d}}{\mathrm{d}t} T_B(t) = \gamma\beta [T_V(t) - T_B(t)], \tag{11}$$

and so

$$T_B(t) = T_V(t) - \frac{1}{\gamma\beta} \frac{\mathrm{d}}{\mathrm{d}t} T_B(t) \tag{12}$$

holds. We now investigate the net effect of the bloodflow due to the described model. Straightforward integration of the source over the computational domain results in

$$\begin{aligned}\int_D Q_{\mathrm{B}}(\mathbf{x},t)\,\mathrm{d}x &= \alpha\left[\beta T_{\mathrm{B}}(t) - \int_D K_{\mathrm{B}}(\mathbf{x})B(\mathbf{x})T(\mathbf{x},t)\,\mathrm{d}\mathbf{x}\right]\\ &\overset{(12)}{=} \alpha\beta T_{\mathrm{V}}(t) - \frac{\alpha}{\gamma}\frac{\mathrm{d}}{\mathrm{d}t}T_{\mathrm{B}}(t) - \alpha\beta T_{\mathrm{V}}(t)\\ &= -\frac{\alpha}{\gamma}\frac{\mathrm{d}}{\mathrm{d}t}T_{\mathrm{B}}(t). \end{aligned} \tag{13}$$

Although result (13) may look surprising at first glance since one might expect that the bloodflow should have zero net effect regardless of the temporal dependence of the temperature of the bloodpool, it neatly illustrates crucial properties of the time-dependent bloodflow model.

In order to demonstrate these properties, we investigate a model situation. Therefore, note that α, β and γ are positive constants. Consider a steady-state situation, i.e. $T_{\mathrm{B}} = T_{\mathrm{V}}$ holds. If the body is heated by a heat source at a boundary, the temperature within the body increases and we see by Equation (9) that T_{V} will increase. By (11) this has the effect that the bloodpool temperature T_{B} will increase in the very next future. When employing this in (13) we get the result that the total of all sources in the body is negative. The described situation has the following meaning: While the blood in the bloodpool cools the increasingly warm body in the mean if the body is exposed to heat, it also takes over heat from it. In the corresponding situation when the body is exposed to cold, the increasingly cold body is warmed in the mean by the blood in the bloodpool which also takes over some of the coldness of the body. The bloodpool and the body are to be seen as two separate systems which are connected via heat fluxes determined by the mentioned equations. Thereby, one can consider the bloodpool as having the function of a regulator.

In the steady-state situation, the temporal derivative of T_{B} is zero and we see by (13) that the two systems are in an equilibrium since the net effect of the bloodfiow is also zero which is a desired result and represents the starting point of the whole argumentation. Furthermore, the model described in Reference [9] is included in the described model. For unsteady computations, the additional equation (8) has to be discretized and integrated within our algorithm.

4. ABOUT THE FINITE VOLUME APPROXIMATION

Within this work we only want to sketch the general idea. We consider the integral form of Equation (7), namely

$$\frac{\mathrm{d}}{\mathrm{d}t}\int_\sigma \bar{T}(\mathbf{x},t)\,\mathrm{d}\mathbf{x} = \int_{\partial\sigma}\left[\frac{\lambda(\mathbf{x})}{k(\mathbf{x})}\nabla\bar{T}(\mathbf{x},t) - \frac{\lambda(\mathbf{x})\bar{T}(\mathbf{x},t)}{k(\mathbf{x})^2}\nabla k(\mathbf{x})\right]\mathrm{d}s + \int_\sigma f(\mathbf{x},t)\,\mathrm{d}\mathbf{x} \tag{14}$$

for all control volumes $\sigma \subset D$. In order to solve (14) numerically by means of a finite volume method, the spatial domain $\bar{D}$ has to be decomposed into a finite number of sub-domains. We start from a conforming triangulation of $\bar{D}$ which is the primary grid, see Figure 1.

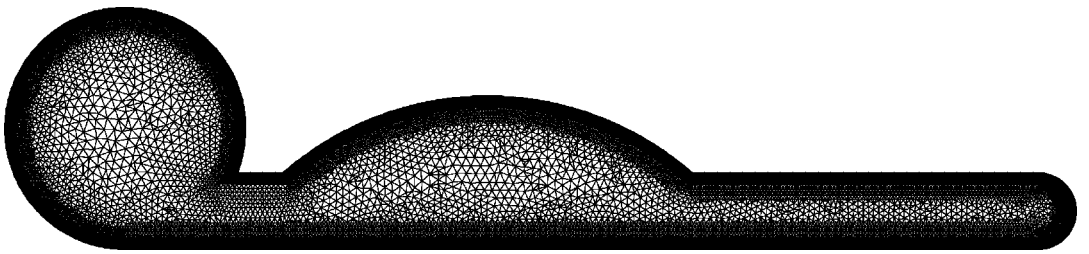

Figure 1. Primary grid.

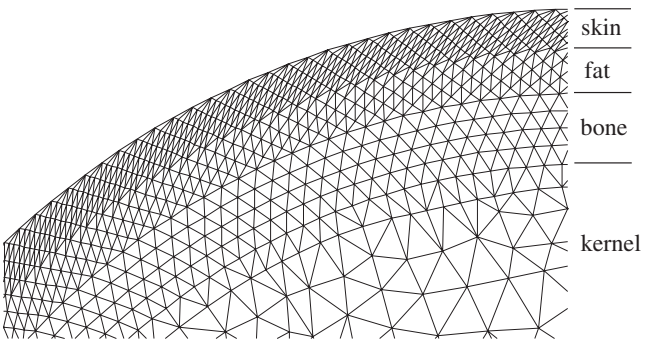

Figure 2. Primary grid in the head region.

For a comprehensive definition of the notion of the primary grid we refer to Reference [14]. In order to achieve an appropriate resolution of the areas which feature skin, fat and bone, we define structured subgrids within these types of tissue, see Figure 2.

The occurring second-order derivatives within Equation (7) require the evaluation of first-order derivatives on the boundary of each control volume. Therefore, we use a secondary mesh where the computation of these derivatives is straightforward. We define a discrete control volume σ_i as the open subset of D which includes the node $\mathbf{x}^{\mathrm{i}}$ and which is bounded by the straight lines defined by the connection of the midpoints of the sides of the triangles adjacent to the $\mathbf{x}^{\mathrm{i}}$ with the barycentres of the corresponding triangles adjacent to these points, see Figure 3. The barycentre of the triangle in the middle is denoted by $\mathbf{x}^{\mathrm{s}}$. Concerning the boundaries, we use basically the same discretization as Fischer *et al.* [9] which does not oppose the use of time-dependent Dirichlet conditions. Thereby sets of boundary temperatures for back, belly, head, neck and legs are defined while the parameters c and ρ are assumed to take the same value on both sides of the physical boundary.

A finite volume scheme applied to our governing equation is a measure to discretize the evolutionary equation (14) for cell averages of the quantity $\bar{T}$ which are defined with the help of the cell average operator

$$(M^h \bar{T})|_\sigma = \frac{1}{|\sigma|} \int_\sigma \bar{T}(\mathbf{x}, t)\, \mathrm{d}\mathbf{x}$$

where $|\sigma|$ denotes the volume of the control volume σ. Since there is not enough space to describe the whole procedure, we only note that the main difference to the scheme used by

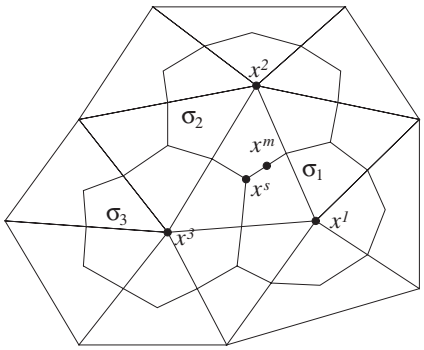

Figure 3. The secondary mesh.

Fischer *et al.* is the additional discretization of Equation (8). This is done in an explicit way by the approximation

$$\frac{\mathrm{d}}{\mathrm{d}t} T_{\mathrm{B}}(t)|_{t^n} \approx \frac{T_{\mathrm{B}}(t^{n+1}) - T_{\mathrm{B}}(t^n)}{\Delta t}$$

by evaluating all other terms at the current time level and with $T_{\mathrm{B}}(t_0) = T_{\mathrm{V}}(t_0)$ as initial condition. The discussed analytical attributes of the bloodflow model naturally take over to the discrete model. We omit the proof because it only requires summation over mean values of cells instead of integration over the domain and is a straightforward discrete representation of the proceeding in the analytical case.

Comparisons of the scheme used in Reference [9] with analytical steady-state solutions have successfully been done recently [16] in order to prove the practical validity of the numerical method, while theoretical investigations have already shown that the scheme satisfies a discrete minimum–maximum-principle [9].

5. NUMERICAL SIMULATIONS

We now present some typical results for the described model. We use the mesh illustrated in Figure 1 which displays the mesh for an infant of weight 1000 g. The triangulation is composed of about 37 000 triangles and 19 000 control volumes. It features structured subgrids as described in Figure 2.

Comparisons of steady-state results computed with our scheme with results used in Reference [9] have shown that we get the same steady-state solutions. One of such solutions is displayed by the top picture of Plate 1. This picture shows the temperature distribution resulting from 299.15 K at the boundaries of the head section while the temperature at the rest of the boundary is given by comfortable 309.15 K. Plate 1 shows the evolution of the physical states from the described state at the top to the state corresponding to the picture at the bottom when employing 299.15 K at head, neck and back while holding 309.15 K at the rest of the boundary. This choice represents the situation that a cooling influence at the boundary is comparable to the influence of the source terms. It also represents a cooling influence which is in the medical sense only applicable for a short time since otherwise the health of the infant would be in danger. These physical states are taken 3, 21 and 60 min after these

boundary conditions are employed. The results show that the brain cannot be cooled down to a great extent while a comfortable temperature for the rest of the body can be provided.

6. CONCLUSION

A finite volume method for the time-accurate simulation of the thermoregulation of premature infants has been presented. Sophisticated models for blood flow, thermal maturity and metabolic heat production together with different body tissues are coupled in an instationary formulation. For the first time, unsteady simulations on that base are done for a premature infant. The presented model provides an excellent base for further applications in the field of thermoregulation and for extensions to the important three-dimensional case.

ACKNOWLEDGEMENTS

The authors would like to thank Dr Jochim Koch and Dr Rainer Kunz, Drägerwerk AG, Department of Basic Development, for their support concerning the modelling process and their keen interest in the study. We would also like to thank Dr Ottmar Bußmann for doing fundamental work in the modelling of thermoregulation of premature infants. Furthermore, we wish to thank Dr Oliver Friedrich for providing his excellent grid generator and Dr Daniel Hempel for his practical help in the visualization process.

REFERENCES

1. Mallard EC *et al*. Neuronal damage in the developing brain following intrauterine asphyxia. *Reproduction, Fertility and Development* 1995; **7**:647–653.
2. Gluckman PD, Williams CE. When and why do brain cells die? *Developmental Medicine and Child Neurology* 1992; **34**:1010–1014.
3. Busto R *et al*. The importance of brain temperature in cerebral ischemic injury. *Stroke* 1989; **20**:1114–1134.
4. Bußmann O. Modell der Thermoregulation des Früh- und Neugeborenen unter Einbeziehung der thermischen Reife. *Ph.D. Thesis*, Medical University of Lübeck, 2000.
5. Webb P, Werner J. A six-cylinder model of human thermoregulation for general use on personal computers. *Annals of Physiological Anthropology* 1993; **12**(3):123–134.
6. Fiala D, Lomas KJ, Stohrer M. A computer model of human thermoregulation for a wide range of environmental conditions: the passive system. *Journal of Applied Physiology* 1999; **87**(5):1957–1972.
7. Loziichuk NG, Onopchuk YN. Mathematical models of the thermoregulation system of the organism and their analysis. *Cybernetics and Systems Analysis* 1995; **34**(4):605–617.
8. Thomas K. Thermoregulation in neonates. *Neonatal Network* 1994; **13**(2):15–22.
9. Fischer B, Ludwig M, Meister A. An application of the finite volume method to the thermoregulation of infants. *BIT* 2001; **41**(5):950–966.
10. Buse M, Werner J. Temperature profiles with respect to inhomogeneity and geometry of the human body. *Journal of Applied Physiology* 1988; **65**(3):1110–1118.
11. Simbruner G. *Thermodynamic Models for Diagnostic Purposes in the Newborn and Fetus.* Facultas Verlag: Vienna, 1983.
12. Holliday MA. Metabolic rate and organ size during growth from infancy to maturity and during late gestation and early infancy. *Pediatrics* 1971; **47**(1)(suppl. 2):169ff.
13. Werner J. Thermoregulatory models. *Scandinavian Journal of Work Environment and Health* 1989; **15**(suppl. 1): 34–46.
14. Breuß M, Fischer B, Meister A. The mathematical modeling of blood flow and its application. In *Proceedings of the International Symposium on Algorithms for Approximation IV*, Huddersfield, 2001.
15. Sonar T. On the construction of essentially non-oscillatory finite volume approximations to hyperbolic conservation laws on general triangulations: polynomial recovery. Accuracy and stencil selection. *Computational Methods in Applied Mechanical Engineering* 1997; **140**:157–181.
16. Breuß M, Dolejší V, Meister A. On an adaptive method for heat conduction problems with boundary layers. *Hamburger Beitraege zur Mathematik*, 2001; available at http://www.math.unihamburg.de/math/research/preprints/hbamf.html.

